

Ultrafast Time-Resolved Contrast-Enhanced 3D Pulmonary Venous Cardiovascular Magnetic Resonance Angiography Using SENSE Combined with CENTRA-Keyhole

Hermann Körperich, PhD,¹ Jürgen Gieseke, MSc,² Hermann Esdorn, MD,¹ Andreas Peterschröder, MD,¹ Romhild Hoogeveen, PhD,² Peter Barth, MSc,¹ Matthias Peuster, MD,³ Hans Meyer, MD,^{1,3} Samir Sarikouch, MD,³ and Philipp Beerbaum, MD^{1,3}

Institute for Magnetic Resonance Imaging, Ruhr-University of Bochum, Bochum, Germany¹

MR Clinical Science, Philips Medical Systems, Best, The Netherlands²

Clinic for Congenital Heart Disease, Heart and Diabetes Center Northrhine-Westfalia, Ruhr-University of Bochum, Bochum, Germany³

ABSTRACT

Purpose: To evaluate the diagnostic benefit of time-resolved CENTRA-keyhole contrast-enhanced cardiovascular magnetic resonance angiography (CE-CMRA) for improving arterial-venous separation of pulmonary vessels. **Methods:** Twenty-three patients (18 males; age = 58 ± 11 y) after radiofrequency pulmonary vein isolation to treat atrial fibrillation were examined using CENTRA-keyhole based multi-phase 3D CE-CMRA yielding 6 near-isotropic 3D datasets every 1.6 s (50–60 coronal partitions, $1.4 \times 1.4 \times 1.3$ mm, SENSE-factor 3). Results were compared with conventional non-keyhole CE-CMRA (identical parameters, SENSE-factor 2). **Results:** Data acquisition was accelerated by a speedup factor of ~ 9 compared with the reference CE-CMRA (SENSE 1.5*, keyhole 6*). No pulmonary venous stenoses were detected by either method, overall pulmonary venous diameters were 17.1 ± 3.6 mm. Applying Bland-Altman analysis, vessel diameters differed by a mean of $0.1 \text{ mm} + 2.1 \text{ mm}/-2.0 \text{ mm}$ (mean ± 2 SD), indicating close agreement between both techniques. Interobserver variability was higher for CENTRA-keyhole (mean = 0.1 mm ; mean ± 2 SD: $+2.5 \text{ mm}/-2.3 \text{ mm}$) compared to conventional technique (0.0 mm ; $+1.6 \text{ mm}/-1.5 \text{ mm}$), corresponding to a percentual deviation (mean ± 2 SD) of the mean diameter of approximately $\pm 15\%$ (keyhole CE-CMRA) and $\pm 10\%$ (conventional CE-CMRA), respectively. Using keyhole-based time-resolved CE-CMRA, the contrast between pulmonary veins versus aorta/pulmonary artery was significantly increased ($p < 0.05$), which improved vessel depiction. In 12 cases, the contrast bolus arrival was delayed in one of the pulmonary veins by 1 dynamic frame (= 1.6 seconds); in 7 cases by 2 frames (= 3.2 seconds) and in 1 subject by 3 frames (= 4.8 seconds). The bolus usually appeared first in the upper right pulmonary vein whereas a delay occurred most often in the lower left pulmonary vein. **Conclusions:** Conventional CE-CMRA may be advantageous for accurate vessel size measures as evidenced by superior interobserver reproducibility in this study. Multi-dynamic CE-CMRA using CENTRA-keyhole with SENSE, however, allows for improved arterio-venous separation of pulmonary vessels and additional dynamical information on pulmonary venous perfusion, while maintaining high spatial resolution. Exact bolus timing is no longer needed.

Received 10 August 2005; accepted 4 June 2006.

Keywords: Magnetic Resonance Angiography, Pulmonary Veins, Time-Resolved, Contrast-Enhanced, Keyhole.

Correspondence to: Hermann Körperich, PhD, Institute for Magnetic Resonance Imaging and Clinic for Congenital Heart Disease, Heart- and Diabetes Center, Nordrhein-Westfalen, Ruhr-University of Bochum, Georgstr. 11, D-32545 Bad Oeynhausen, Germany
tel.: +49-(0)5731-97-1845; fax: +49-(0)5731-97-1862
email: hkoerperich@hdz-nrw.de

INTRODUCTION

Noninvasive angiography of thoracic vessels has greatly been improved with the introduction of contrast-enhanced 3D cardiovascular magnetic resonance angiography (CE-CMRA) (1). The method allowed to overcome the limitations of traditional methods such as time-of-flight cardiovascular magnetic resonance angiography (CMRA) and phase-contrast CMRA (2). Over the past decade, CE-CMRA has evolved as a firmly established imaging technique in the diagnosis of a variety of pulmonary vascular pathologies such as pulmonary embolism, sequestration (3), arterio-venous malformations (4, 5) and pulmonary vein stenosis (4).

The non-invasive technique has become especially valuable in diagnosis and postoperative follow-up of patients with congenital abnormalities of pulmonary arterial blood supply (7, 8) and pulmonary venous anomalies (9–11). However, overlay of thoracic vessels may at times limit the diagnostic value. Separation of pulmonary and aortic vessels is possible if the scan time is not longer than the pulmonary transit time of ~ 7 s (12). With a large 3D volume scanned at high-spatial-resolution, this can only be achieved when using undersampling techniques such as half-fourier imaging and parallel imaging (13–15). Even so, one is still left with overlay of pulmonary arteries and veins when imaging the pulmonary vasculature. This may hamper diagnosis in clinical conditions with rapid or inhomogeneous bolus transit times (4, 5) or complex pulmonary perfusion pathology such as with multifocal blood supply in congenital heart disease (7). To improve on this problem, one would have to reduce scan times to less than 2 s (16) while maintaining the spatial resolution and volume coverage. Although a variety of multiphase 3D CE-CMRA protocols were recently introduced (16–18), none of them achieved this request at high-spatial-resolution in a large volume. The best approach in terms of temporal resolution was published by Fink et al. and yielded a temporal resolution of 1.48 s at a voxel size of $4.4 \times 2 \times 5$ mm (19), which is, however, not good enough for precise anatomical diagnoses.

We, therefore, sought to evaluate a novel CE-CMRA technique using a combination of SENSE and CENTRA-keyhole to drastically speed up data acquisition at high-spatial-resolution as proposed by Hooegeveen et al. (20). This may allow for additional dynamic information on the time course of blood supply in patients with different pulmonary vascular territories in only one single breathhold. Potential applications include visualization of aortopulmonary shunts, partial anomalous pulmonary venous returns, arterio-venous vessel malformations and multifocal blood supply in congenital heart disease.

We hypothesized that: time-resolved rapid 3D CE-CMRA scanning offers improved separation between pulmonary arteries and veins without exact bolus timing; and variability in vessel diameter measurements is comparable to conventional CE-CMRA.

For validation purpose, the hypotheses were tested in the clinical setting of pulmonary venous angiography in patients who underwent a radiofrequency ablation to treat atrial fibrillation.

MATERIALS AND METHODS

Study population

A total of 23 patients (5 females) after an electrophysiological study using radiofrequency pulmonary vein isolation to treat atrial fibrillation underwent CMRA to rule out postprocedural pulmonary venous stenoses by assessing the dimensions of the pulmonary veins as well as the pulmonary venous architecture. Mean patient age was 58 ± 11 years. All patients were in functional class NYHA (New York Heart Association) I or II, and no patients had overt heart failure. Sinus rhythm was present in 20 of 23 patients. The study was approved by the local Ethics Institutional Review Committee and informed written consent was obtained from the participants.

Cardiovascular magnetic resonance

All examinations were performed on a clinical 1.5 Tesla whole body magnetic resonance scanner (ACS-NT, R10, maximum gradient performance 30 mT/m, slew rate 150 T/m/s, Philips Best, the Netherlands). The body coil was used for signal transmission and a 5 element cardiac phased-array surface coil for signal detection. Plan scans in 3 orthogonal planes used non ECG-triggered balanced gradient-echo (TR/TE/flip = 2.2 ms/1.1 ms/55°) to allow positioning of the 3D volume of the subsequent angiographic scans. A free-breathing SENSE reference scan (<1 minute scan time) was performed to obtain sensitivity information necessary for application of the SENSE technique (13).

A multi-dynamic non-ECG-triggered 3D T1w gradient-echo with CENTRA technique (21) was combined with keyhole technique (keyhole CE-CMRA), where only the central part is repeated several times and periphery of k-space is completed using the appropriate data of a subsequent reference dataset (20).

The central sphere (keyhole = central 15% of k-space) was sampled 6 times in a row every 1.6 s, followed by a 9 s reference dataset to finally reconstruct a total of six high-resolution 3D datasets (20). Total imaging time was 18.6 s (= 6×1.6 s + 9 s) which allowed data collection in one single breathhold. Volume coverage was achieved by 50–60 partitions using overcontiguous slice in the coronal plane resulting in an effective partition thickness of 1.3 mm. A field-of-view (FOV) of 530 mm and matrix of 368×368 yielded a near-isotropic voxel size of $1.4 \times 1.4 \times 1.3$ mm for the reference and for the previously acquired dynamic frames after k-space completion. We used TR/TE/flip = 3.2 ms/1.1 ms/30° with half-Fourier acquisition. For keyhole-CE-CMRA a SENSE reduction factor (SF) of 3 was applied in the left-right phase reduction direction.

These time-resolved keyhole-based CMR angiograms were compared with conventional CE-CMRA (no keyhole) obtained with non ECG-triggered 3D T1w gradient-echo technique as routinely used in our institute for delineation of the pulmonary venous anatomy. All parameters were kept identical (including use of the CENTRA technique), except for the use of a SENSE reduction factor of only 2 (instead of 3), resulting in a scan duration of 13.8 s.

A preceding multi-dynamic single slice T1w gradient-echo sequence with TR/TE/flip=1.8 ms/0.6 ms/30° and a slice thickness of 120 mm, providing low resolution images every 175 ms, was used to register contrast bolus arrival for proper timing of the subsequent CE-CMRA scan. CENTRA-keyhole preceded conventional CE-CMRA in 10 cases, and vice versa in 13 cases. Data acquisitions were separated from each other by a time interval of 5 minutes.

Echocardiography

Echocardiography was performed to assess right and left heart chamber sizes and function as well as to screen for valvular defects and thrombi.

Contrast agent

For all CE-CMRA protocols, injections at a flow rate of 2.5 mL/s were performed with an automated power injector (Spectris Solaris, Medrad, Volkach, Germany) using 8 mL of a gadolinium-based contrast agent (0.5 mol/L MULTIHANCE, Bracco Altana Pharma GmbH, Konstanz, Germany) followed by 30 mL of saline flush at 2.5 mL/s flow rate.

MRA data analysis

The image analysis was performed independently by two experienced CMR radiologists (A.P., H.E.). The quantitative assessment included the determination of the dimensions of the four pulmonary veins at the smallest size prior to their entrance into the left atrium (Fig. 1) as well as calculation of the vessel contrast. For this, regions of interest (ROIs) were placed in each of the following vessels: left pulmonary artery (cross section), aortic arch (cross section) and the atrial entrance of each of the four pulmonary veins. The size of the ROIs was chosen in order to cover as much of the vascular lumen as possible and to carefully exclude voxels containing partial volume information. The lack of non-filtered image data made it impossible to obtain accurate noise measurements in air as necessary for “true” contrast-to-noise calculations. We, therefore, defined image contrast using the following formula:

$$\text{contrast} = \frac{|SI_A - SI_B|}{|SI_A + SI_B|} \quad [1]$$

with SI = signal intensity measured in the ROI of the corresponding vessel A and B, respectively (22). To avoid misleading contrast values in case of temporal non-occurrence of contrast agent in the considered pulmonary vein, only signal intensity values exceeding half of the signal maximum (= threshold) found in the time-resolved keyhole CE-CMRA data were accepted, ensuring sufficient vessel delineation (Due to the formular characteristics—modulus of the numerator and denominator—it is theoretically possible that high contrast values could be achieved if no contrast media is present in the vessel of interest [= invisible pulmonary veins] but some already in the pulmonary artery).

Vessel size measurements were performed on: double-oblique paracoronal maximum intensity projections (MIPs); and

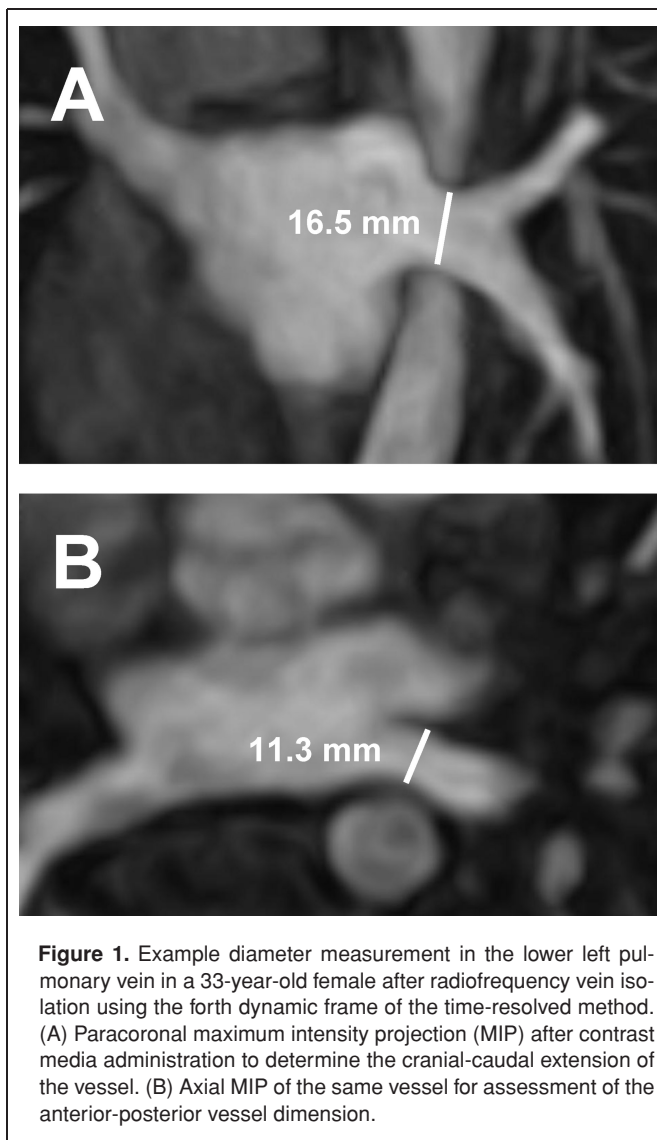


Figure 1. Example diameter measurement in the lower left pulmonary vein in a 33-year-old female after radiofrequency vein isolation using the forth dynamic frame of the time-resolved method. (A) Paracoronal maximum intensity projection (MIP) after contrast media administration to determine the cranial-caudal extension of the vessel. (B) Axial MIP of the same vessel for assessment of the anterior-posterior vessel dimension.

axial MIPs with a slab thickness of 5 mm. The smallest possible extension of the vessel distal to the ostium was defined as diameter in each of the two MIPs, yielding two measures (cranial-caudal and anterior-posterior direction) per vessel (Fig. 1).

Statistical analysis

Mean values, standard deviation and range were computed for evaluation of contrast differences between the vessels for both CE-CMRA techniques. Significance of the observed differences was tested with a paired Student t-test. A chi square test was applied for comparing the differences in bolus arrival times in the pulmonary veins. A p value of ≤ 0.05 was considered as statistically significant. The analysis of Bland and Altman (23) was used to quantify the agreement between conventional and time-resolved keyhole CE-CMRA vessel lumen measurements and to determine interobserver variability. Minimal stenosis detectable with 95% certainty was estimated by percentage deviation from the calculated mean values of the

absolute pulmonary vein diameters found by the two observers. Image quality and vascular delineation were subjectively analyzed using a three-point scale: I = keyhole CE-CMRA superior to conventional CE-CMRA; II = comparable quality; and III = conventional CE-CMRA superior to keyhole CE-CMRA. Kappa statistics were used to estimate interobserver agreement with interpretation of the κ -values according to Altman (weak: ≤ 0.2 ; fair: 0.2–0.4; moderate: 0.4–0.6; high: 0.6–0.8; very high: 0.8–1.0) (24).

RESULTS

All scans were completed successfully. Image quality was satisfactory in all patients with both time-resolved keyhole CE-CMRA and conventional CE-CMRA. No pulmonary venous stenoses were diagnosed in any of the patients by the two independent observers using either technique. The dynamic part of the 3D CMRA data collection was accelerated by a speedup factor of 9 compared with the reference CE-CMRA protocol. Figure 2 shows five representative MIPs of time-resolved keyhole CE-CMRA, compared with the conventional technique.

Keyhole versus conventional CE-CMRA: Vessel lumen measures, interobserver test, subjective image quality

The right upper, right lower and left upper pulmonary veins had a mean diameter ranging from 16.4 mm to 19.2 mm applying conventional CE-CMRA and 16.6 mm to 19.4 mm for CENTRA-keyhole CE-CMRA, respectively. The left lower pulmonary vein had a mean diameter in anterior-posterior direction

Table 1. Comparison of the mean pulmonary vein diameter \pm standard deviation (maximum; minimum values) applying conventional and CENTRA-keyhole CE-CMRA, respectively

	Conventional CE-CMRA	CENTRA-Keyhole CE-CMRA
RUPV		
cc	18.5 \pm 2.7 (24.0; 12.6)	18.9 \pm 2.8 (24.2; 13.0)
ap	17.6 \pm 3.0 (23.3; 11.2)	17.6 \pm 3.9 (24.5; 10.2)
RLPV		
cc	18.3 \pm 2.8 (24.3; 13.3)	17.8 \pm 2.5 (22.3; 13.1)
ap	16.4 \pm 3.3 (26.0; 10.7)	16.6 \pm 3.1 (23.8; 9.5)
LUPV		
cc	19.2 \pm 3.0 (23.0; 13.0)	19.4 \pm 2.8 (23.5; 13.2)
ap	17.0 \pm 3.3 (23.7; 11.7)	17.4 \pm 3.2 (23.7; 11.3)
LLPV		
cc	17.3 \pm 2.2 (20.9; 13.3)	17.3 \pm 2.0 (20.3; 14.2)
ap	11.7 \pm 2.7 (17.2; 7.2)	11.7 \pm 3.1 (18.2; 7.1)

All values in mm. cc = measures in cranial-caudal direction; ap = measures in anterior-posterior direction.

of 11.7 mm by either method (Table 1). This would result in an overall mean pulmonary venous diameter of 17.0 \pm 3.6 mm (mean \pm SD) for conventional and 17.1 \pm 3.6 mm for CENTRA keyhole CE-CMRA, respectively.

Bland-Altman statistics demonstrated good agreement between both angiographic methods for depiction of vessel lumen measures. Negligible mean differences of 0.1 mm with limits of agreement (mean \pm 2SD) between -2.0 to $+2.4$ mm were found by both observers (Fig. 3). Confidence intervals (c.i.) were $+2.1$ to $+2.7$ mm and -1.9 to -2.6 mm for observer 1, and $+1.9$ to $+2.4$ mm and -1.7 to -2.2 mm for observer 2, respectively.

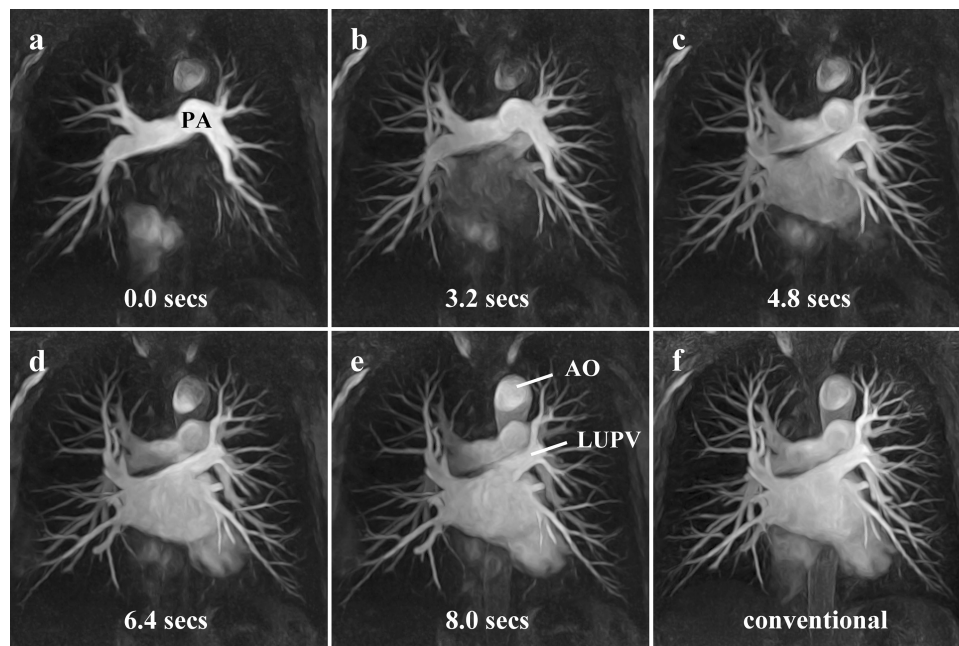
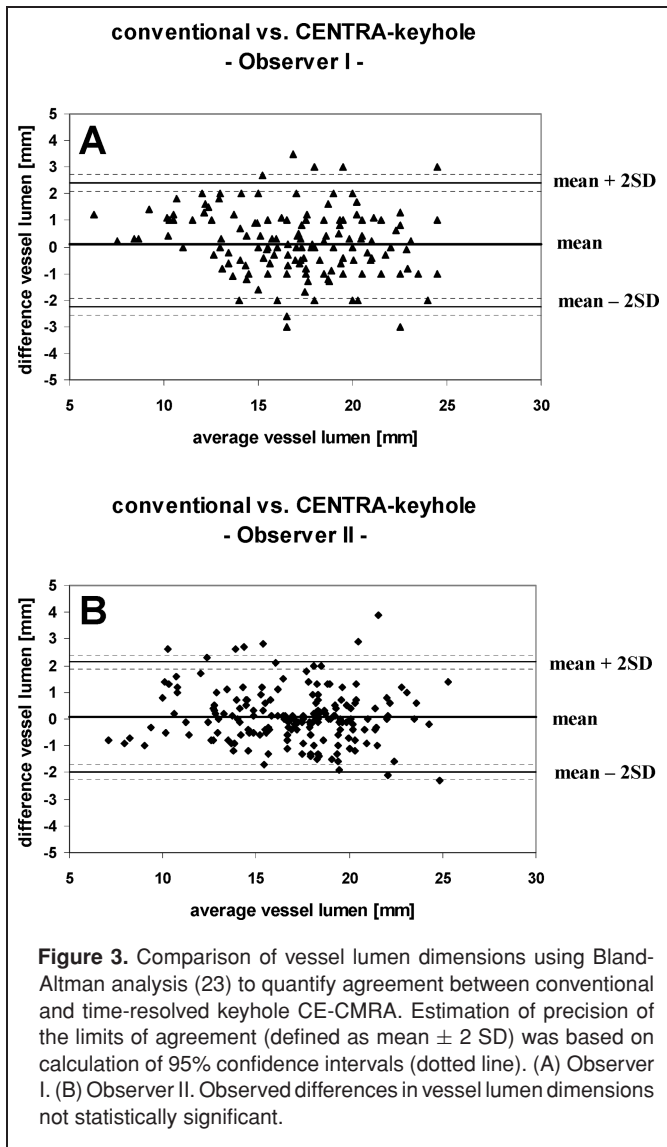
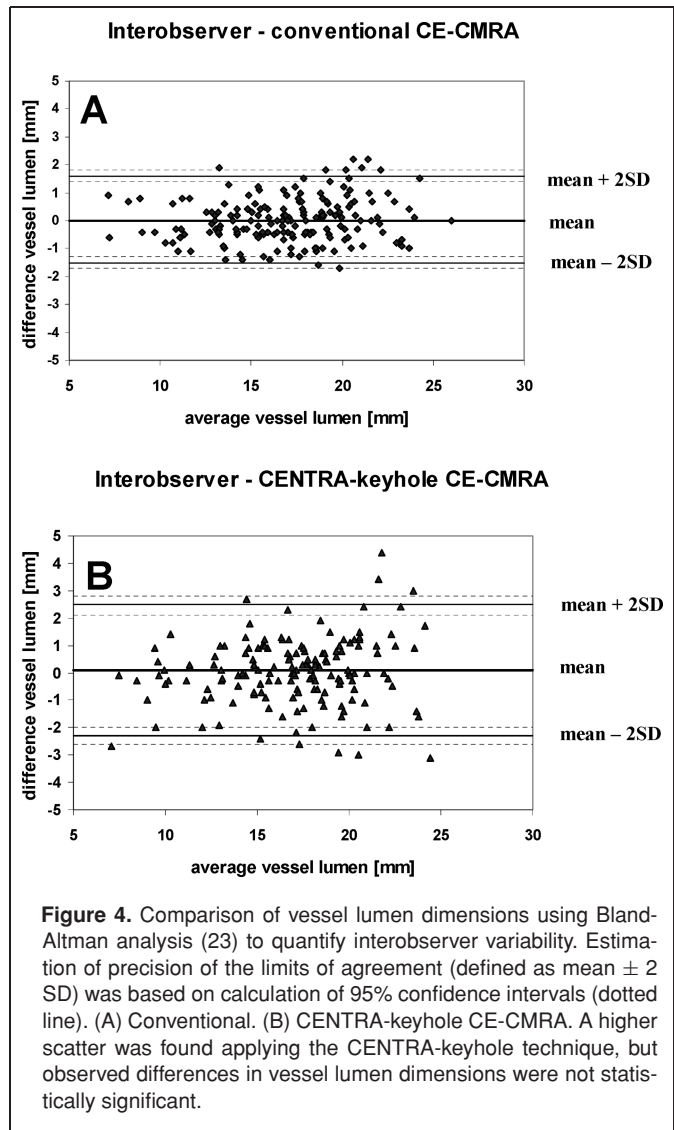


Figure 2. Time-resolved pulmonary 3D-CMRA using CENTRA-keyhole with SENSE (a–e) demonstrating vessel filling. Signal maximum is first visible in upper left pulmonary vein; (f) conventional CE-CMRA. PA = pulmonary artery, AO = aorta, LUPV = left upper pulmonary vein.



Regarding interobserver variability, almost no mean differences were observed for conventional (mean = 0.0 mm) and time-resolved keyhole CE-CMRA (mean = 0.1 mm), respectively (Fig. 4). However, limits of agreement were higher (-2.3 to +2.5 mm; c.i.: +2.1 to +2.8 mm and -2.0 to -2.6 mm) when applying keyhole CE-CMRA as compared to the conventional technique (-1.5 to +1.6 mm; c.i.: +1.4 to +1.8 mm and -1.3 to -1.7 mm). Accordingly, expressed in percentages, the mean diameter bias between both observers as calculated by the Bland-Altman approach was 0% for either technique. Limits of agreement (mean \pm 2SD), however, were only -9.5 to +9.6% (c.i.: +8.4 to +10.8% and -8.3 to -10.7%) by conventional CE-CMRA, but -14.6 to +14.9% (c.i.: +12.9 to +16.9% and -12.7 to -16.6%) for CENTRA keyhole CE-CMRA (Fig. 5). Theoretically, if these limits of agreement were related to the overall pulmonary venous mean diameter of 17.0 mm and 17.1 mm, respectively, as calculated above, the total range of 2SD above and 2SD below this mean values would result in a observer variation

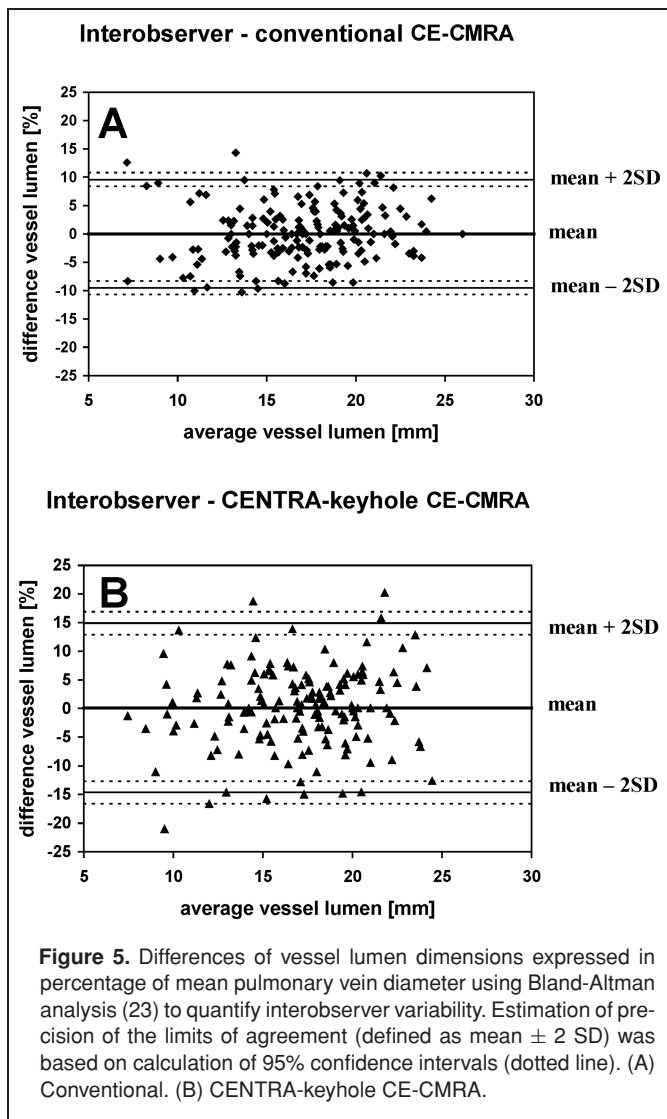


(4SD) in the order of 29.5% (-14.6% to +14.9%) for keyhole CE-CMRA, but only 19.1% (-9.5% to +9.6%) for conventional CE-CMRA. All calculated differences were statistically not significant.

The results of the subjective analysis of the image quality revealed no obvious image degrading by use of the keyhole technique with high interobserver agreement ($\kappa = 0.61$). With respect to the succession of the applied CMRA methods (keyhole prior or after conventional CE-CMRA), no obvious limitation of the angiographical quality due to the preceding contrast agent injection was observed for either technique.

Keyhole versus conventional CE-CMRA: Vessel contrast

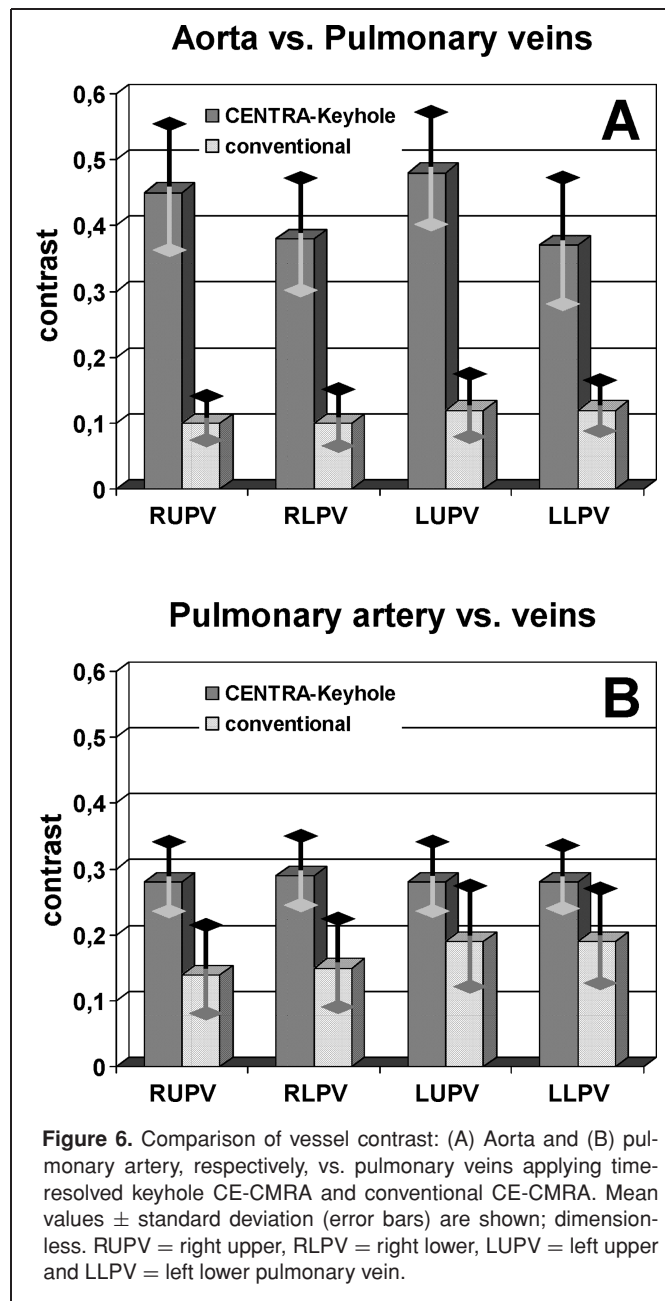
Applying keyhole CE-CMRA, we found mean arterial-venous contrast values between right upper, right lower, left upper and left lower pulmonary vein and the pulmonary artery of approximately 0.28 ± 0.11 , whereas corresponding contrast



values for conventional CE-CMRA were significantly lower and ranged between 0.14 ± 0.14 and 0.19 ± 0.16 ($p \leq 0.05$) (Fig. 6). Comparing the four pulmonary veins and the aortic arch, mean arterial-venous contrast values ranged between 0.38 ± 0.18 and 0.48 ± 0.18 for time-resolved keyhole CE-CMRA, while for conventional CE-CMRA the contrast was again significantly lower, ranging between 0.10 ± 0.07 and 0.12 ± 0.10 ($p \leq 0.05$).

Additional dynamic information by keyhole CE-CMRA

In order to estimate any potential differences in vascular filling characteristics of the pulmonary vasculature, we determined the respective arrival times of the observed signal maximum in each of the four pulmonary veins as outlined in Table 2. To avoid any bias resulting from different onset time points of the angiographic sequence, a relative comparison was performed. A simultaneous appearance of the contrast bolus in all pulmonary veins was found in only 3 of the 23 cases. In 12 cases arrival was delayed in one of the considered vessels by one dynamic



frame, corresponding to a temporal offset of 1.6 s; in 7 cases by 2 dynamic frames (3.2 s); and in 1 subject by 3 dynamic frames (4.8 s). Furthermore, Table 2 reveals that in the majority of subjects the contrast bolus arrives first in the upper right pulmonary vein, whereas in the lower left pulmonary vein contrast agent appearance seems to be delayed in this study population. The differences in bolus arrival times were statistically significant for right upper pulmonary veins (RUPV) vs. both lower pulmonary veins and for left upper (LUPV) vs. left lower pulmonary veins (LLPV).

To estimate pulmonary transit times, we determined the maximum delay of signal (= bolus) appearance between the pulmonary artery (reference in time) and bolus arrival in one of the pulmonary veins. As outlined in Table 2, transit times ranged

Table 2. Relative arrival time of the signal maximum in each of the 4 pulmonary veins as derived from signal-intensity vs. time curves

No.	RUPV	RLPV	LUPV	LLPV	max. PV delay [s]	ECG	Echo	Transit time [s]
1	1	1	1	2	1.6	SR	a	1.6
2	2	2	2	1	1.6	SR	a	3.2
3	1	1	2	2	1.6	A. fib.	a	1.6
4	1	1	1	2	1.6	SR	a	8.0
5	1	2	1	3	3.2	A. fib.	b	6.4
6	1	2	1	3	3.2	SR	b	3.2
7	1	2	1	3	3.2	SR	a	8.0
8	1	3	3	3	3.2	SR	b	6.4
9	1	1	2	2	1.6	SR	b	6.4
10	1	3	2	2	3.2	SR	b	4.8
11	1	1	1	1	0.0	SR	b	1.6
12	1	1	1	2	1.6	SR	a	6.4
13	1	2	2	1	1.6	SR	b	1.6
14	1	2	1	1	1.6	SR	b	1.6
15	3	2	1	3	3.2	SR	a	4.8
16	1	1	1	2	1.6	SR	b	3.2
17	1	1	1	1	0.0	SR	b	4.8
18	1	1	1	2	1.6	SR	b	3.2
19	1	2	1	1	1.6	A. fib.	c	1.6
20	1	1	1	4	4.8	SR	b	6.4
21	1	1	1	1	0.0	SR	N/A	3.2
22	1	2	2	3	3.2	SR	N/A	6.4
23	1	2	1	1	1.6	SR	N/A	6.4
Position								
1	21	11	16	8				
2	1	10	6	8				
3	1	2	1	6				
4	0	0	0	1				

Note: SR = normal sinus rhythm; A. fib. = arterial fibrillation; a = no further cardiac impairment; b = normal left ventricular function, atrial dilatation; c = reduced left ventricular function, atrial dilatation; ECG = electrocardiogram; Echo = echocardiography. RUPV = right upper, RLPV = right lower, LUPV = left upper, LLPV = left lower pulmonary vein. The value "1" means contrast bolus first of all visible; position "2" means contrast bolus appears delayed by one frame (= 1.6 s); position "3" means delay of two frames (= 3.2 s) and position "4" means delay of three frames (= 4.8 s). The sixth column represents the maximum temporal delay between first and latest bolus arrival within the pulmonary veins, whereas the seventh column shows the maximum delay between the latest bolus arrival in the pulmonary veins and the left pulmonary artery. In the lower part of the table, the occurrence of the various appearance positions is displayed, indicating physiological pulmonary differences.

between 1.6 to 8.0 s (mean = 4.4 s) in this study population, but no correlations with cardiac function and/or cardiac rhythm were evident.

DISCUSSION

In this study we sought to validate a novel approach to obtain a series of large near-isotropic 3D contrast-enhanced cardiac magnetic resonance angiography volumes every 1.6 seconds by use of SENSE and CENTRA-keyhole. If compared with the reference CE-CMRA technique without keyhole, the dynamic part of the 3D CMRA data collection was accelerated by a total speed-up factor of ~9.

Independent from the applied angiographic technique, pulmonary venous diameters ranged between 17.3 to 19.4 mm in the cranial-caudal and between 11.7 to 17.6 mm in the anterior-posterior (AP) direction, respectively. These measures are con-

sistent with those found by Syed et al. (AP: 14.1–16.1 mm) in their study comparing 2D cine CMR with 3D CMRA (27). Regarding the results of distance measures, no tendency for over- or underestimation was found by each of the two readers applying the CENTRA keyhole method as indicated by the negligible bias of 0.1 mm.

Differences between time-resolved CENTRA-keyhole and conventional CE-CMRA

In contrast to the visual grading of the overall image quality, where high interobserver agreement ($\kappa = 0.61$) was found, the limits of agreement of the quantitative diameter measurements reveal a higher scatter for keyhole CE-CMRA (−2.3 to +2.5 mm, as opposed to −1.5 to +1.6 mm for the conventional technique). Thus, it should be emphasized that a subjective

assessment of the image quality is of minor significance for comparing the two methods compared with the more objective calculation of the interobserver reproducibility. Furthermore, the percental interpretation of the scatter reveals that deviations of less than $\pm 15\%$ for dynamic CE-CMRA and less than $\pm 10\%$ for conventional CE-CMRA of the mean pulmonary vein diameter may be introduced by different vessel border interpretation by independent observers and have to be considered for graduation of the severity of stenosis. Nevertheless, despite the inferiority of the CENTRA-keyhole technique in this respect, we regard this source of error still as acceptable, because only diameter reductions of more than 25% are generally considered as hemodynamical relevant in the literature (25).

Several reasons may be responsible for the higher interobserver scatter when applying CENTRA-keyhole CE-CMRA. A slightly reduced vessel sharpness (blurring) was occasionally observed, as shown in the original cross-sectional images in Figure 7. Increased blurring may theoretically be secondary to two different aspects of the keyhole image acquisition strategy. Firstly, a rapid contrast decrease when traveling to the periphery of k-space (reference scan) may induce blurring artifacts because contrast agent has to be present both in the dynamic and in the reference part. Secondly, the restricted amount of acquired data to fill the central part in k_y, k_z -space may also contribute to some blurring although image quality might theoretically benefit from high temporal resolution using keyhole technique because

misregistration due to long data sampling periods may be reduced (26). Thirdly, the higher SENSE reduction factor of 3 as used with CENTRA keyhole CE-CMRA may have introduced increased noise inhomogeneity (13) as compared with conventional CE-CMRA for which a SENSE reduction factor of only 2 was used. Lastly, for evaluation of vessel lumen dimensions, both observers had a free choice of the utilized dynamic frame, which might have additionally contributed to the scatter.

In summary we could state that angiograms obtained with conventional CE-CMRA tend to result in superior vessel sharpness, as reflected by the higher interobserver reproducibility. The clinical impact of the higher scatter with keyhole CE-CMRA for the quantitative assessment of vessel stenoses remains, however, unclear because such stenoses were not encountered in this study.

Benefits of CENTRA-keyhole 3D CE-CMRA: Reduction of arterio-venous overlay

As shown in this study, vessel contrast was significantly increased between pulmonary veins and the pulmonary artery as well as the aorta when applying dynamic keyhole CE-CMRA. This is explained by the reduction of arterial-venous overlay secondary to the phasic nature of time-resolved CE-CMRA techniques (17) as well as the characteristics of the CENTRA technique (21). Furthermore, due to a temporal resolution of below 2

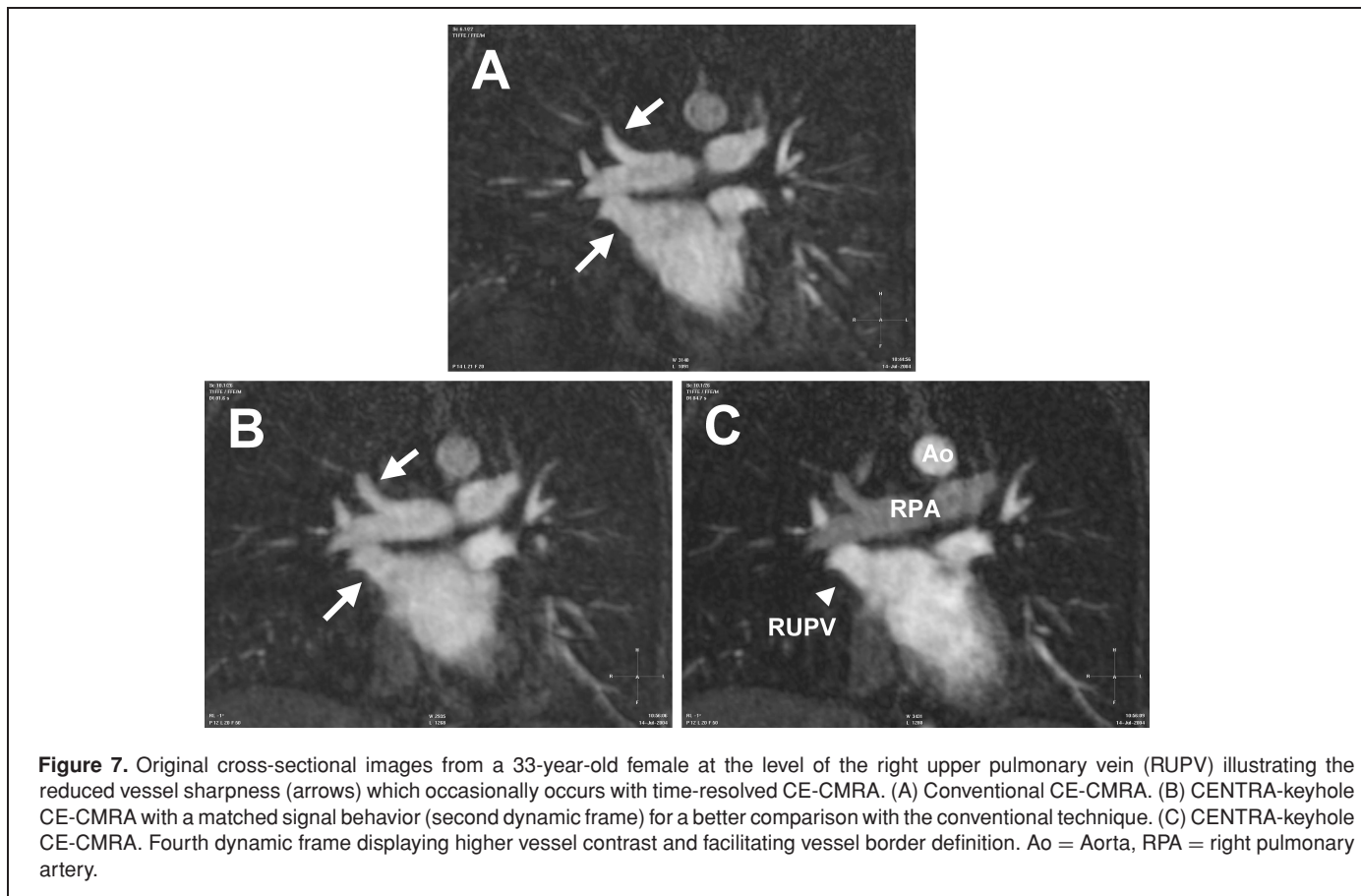


Figure 7. Original cross-sectional images from a 33-year-old female at the level of the right upper pulmonary vein (RUPV) illustrating the reduced vessel sharpness (arrows) which occasionally occurs with time-resolved CE-CMRA. (A) Conventional CE-CMRA. (B) CENTRA-keyhole CE-CMRA with a matched signal behavior (second dynamic frame) for a better comparison with the conventional technique. (C) CENTRA-keyhole CE-CMRA. Fourth dynamic frame displaying higher vessel contrast and facilitating vessel border definition. Ao = Aorta, RPA = right pulmonary artery.

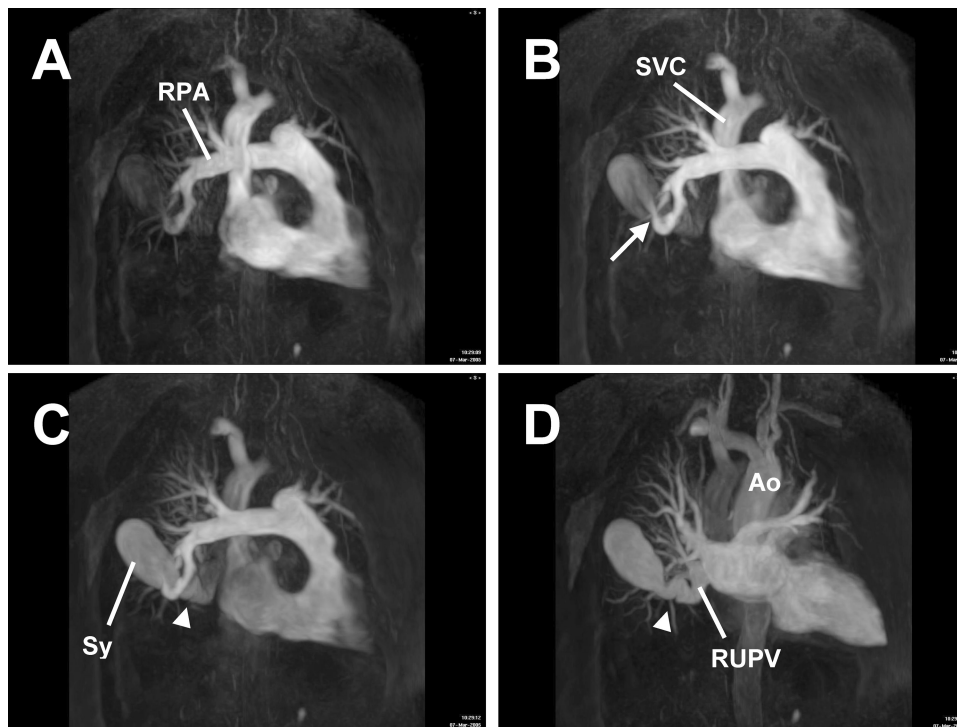


Figure 8. Maximum-intensity-projections from a non-study patient (71 yrs, male) with an arterio-venous syrx (Sy) in the right inferior lobe of the lung. CENTRA-keyhole CE-CMRA with 9 time frames acquired with a temporal resolution of 1.4 s. (A) Third time frame. (B) Fourth time frame, displaying the entry (arrow) and the filling of the contrast media into the syrx. (C) Fifth time frame, showing the onset (arrow head) of contrast media outflow into the right lower pulmonary vein. (D) Ninth time frame, demonstrating the contrast media flow into the left atrium without arterial overlay. The syrx was excised in succession and validated by histology. RUPV = right upper pulmonary veins, SVC = superior vena cava, Ao = aorta, RPA = right pulmonary artery.

seconds, the keyhole technique guarantees data acquisition at an adequate time point (optimal contrast bolus) for optimal vessel filling and thus vessel visualization. As shown in Figure 7, signal behavior of conventional CE-CMRA corresponds to the second dynamic frame of CENTRA-keyhole CE-CMRA, whereas a better vessel border definition was obtained in a later time frame of the novel keyhole technique. Theoretically, this should help to improve the reliability of quantitative measurements compared to the conventional technique, but could not be proven in this study because a gold standard with “true” vessel measures is lacking. Additionally, with keyhole CE-CMRA exact bolus timing is no longer mandatory as compared with monophasic techniques, where inadequate timing results occasionally in low-quality angiograms and may require repetition of the angiography.

Therefore, the clinical implication is mainly that there is now a novel time-resolved noninvasive angiographic technique available to assess pulmonary vascular pathologies with inhomogenous perfusion times such as with arteriovenous malformations (4, 5) or congenital abnormalities of pulmonary arterial blood supply (7). An example is given in Figure 8 demonstrating clearly the time course of the dynamic blood flow into the pulmonary arterio-venous malformation, without any need of time consuming single-slice flow measurements.

Visualization of differential pulmonary perfusion

Another result from this study is that it was possible to detect different pulmonary contrast bolus transit times for each of the pulmonary veins by use of the keyhole CMRA protocol (Table 2). The contrast bolus typically appeared first in the right upper pulmonary vein but somewhat delayed in the left lower pulmonary veins. Moreover, we determined pulmonary transit times with peak signal in the pulmonary artery used as a reference in time. In all examined patients such transit times were less than 8 s (mean = 4.4 s). This corresponds roughly to results observed in healthy volunteers by Shor et al. (12), who found a mean pulmonary transit time of 7.7 s, but defined as the delay between pulmonary artery and ascending aorta. However, the value of this approach may be somewhat limited due to the still restricted temporal resolution of 1.6 s. It was not possible in this study to correlate prolongation of pulmonary “transit times” secondary to impaired cardiac function by echocardiography and/or presence of persistent atrial fibrillation and left atrial dilation (Table 2). Moreover, as none of the examined subjects had relevant pulmonary venous or arterial stenoses, we rather postulate that the observed delays in arrival times are related to physiological variability.

Study limitations

No gold-standard for true accuracy data was available, only interobserver scatter to make decision over superiority of one of the two techniques. As this was mainly a validation study performed in patients without relevant stenotic alterations of their pulmonary venous vasculature although was expected to occur in this study and without any obvious differences in the contrast bolus transit times through the various pulmonary territories related to a specific disease, more sophisticated applications in pulmonary vascular disease are needed to clearly demonstrate the clinical benefits of time-resolved 3D CE-CMRA. No gold-standard for estimation of the pulmonary hemodynamics exists and, hence, no correlation with other techniques such as flow measurements to validate the observed different transit times of the various pulmonary lobes was done in this study. No re-examination of the patients to address interstudy reproducibility of the vessel dimensions and thus the minimal stenosis detectable with contrast-enhanced angiography using interstudy data was performed.

Recommended application fields

In summary, we would suggest that conventional CE-CMRA should be applied mainly if high vessel sharpness without need of any dynamic information is desired such as with delineation of smaller vessels in the lung parenchyma or if large image volumes (e.g., whole thorax) need to be acquired in a short breathhold. The temporal demand of time-resolved CE-CMRA is slightly higher related to the desired number of dynamic frames in addition to the reference data set. This may be crucial in some cases. Otherwise, time-resolved CE-CMRA is advantageous in those situations where hemodynamical information would be desirable and/or arterio-venous overlay would limit the diagnostic yield. Examples include pathological arterio-venous connections, as well as multifocal pulmonary perfusion in congenital heart disease.

CONCLUSIONS

For pulmonary vein diameters the limits of agreement for interobserver variability increases from 19.1% (mean – 2SD to mean + 2SD) for conventional CE-CMRA to 29.5% for time-resolved keyhole CE-CMRA. This lower reproducibility was not obvious with visual assessment of image quality. Otherwise, the keyhole technique is advantageous over conventional CE-CMRA in that vessel contrast is significantly improved and dynamic information such as differential pulmonary perfusion data can be generated, which is not possible by conventional CE-CMRA. In addition, there is no need for accurate bolus timing with CENTRA-keyhole CE-CMRA. This indicates that the two angiographic methods should be used according to the clinical question to be answered: for high accuracy (e.g., monitoring the vessel size over time) conventional CE-CMRA; for hemodynamic information (e.g., assessment of pulmonary vascular pathology or arterio-venous malformation) keyhole CE-CMRA.

REFERENCES

1. Kauczor H. Contrast-enhanced magnetic resonance angiography of the pulmonary vasculature. A review. *Invest Radiol* 1998;33:606–17.
2. Prince M, Narasimham D, Stanley J, Chenevert T, Williams D, Marx M, et al. Breath-hold gadolinium-enhanced MR angiography of the abdominal aorta and its major branches. *Radiology*. 1995;197:785–92.
3. Au V, Chan J, Chan F. Pulmonary sequestration diagnosed by contrast enhanced three-dimensional MR angiography. *Br J Radiol* 1999;72:709–11.
4. Maki D, Siegelman E, Roberts D, Baum R, Gefter W. Pulmonary arteriovenous malformations: three-dimensional gadolinium-enhanced MR angiography-initial experience. *Radiology* 2001;219:243–6.
5. Fink C, Eichhorn J, Bock M. Pulmonary arteriovenous malformation and aortopulmonary collateral imaged by time resolved contrast enhanced magnetic resonance angiography. *Heart* 2002;88:292.
6. Faber L, Vogt J, Heintze J, Peterschroeder A, Esdorn H, Meyer H, et al. Pulmonary vein stenosis after radiofrequency pulmonary vein isolation for atrial fibrillation. *J Am Soc Echocardiogr* 2004;17:491–2.
7. Geva T, Greil G, Marshall A, Landzberg M, Powell A. Gadolinium-enhanced 3-dimensional magnetic resonance angiography of pulmonary blood supply in patients with complex pulmonary stenosis or atresia: comparison with x-ray angiography. *Circulation* 2002;106:473–8.
8. Eichhorn J, Fink C, Bock M, Delorme S, Brockmeier K, Ulmer H. Images in cardiovascular medicine. Time-resolved three-dimensional magnetic resonance angiography for assessing a pulmonary artery sling in a pediatric patient. *Circulation* 2002;106:e61–2.
9. Ferrari V, Scott C, Holland G, Axel L, Sutton M. Ultrafast three-dimensional contrast-enhanced magnetic resonance angiography and imaging in the diagnosis of partial anomalous pulmonary venous drainage. *J Am Coll Cardiol* 2001;37:1120–8.
10. Greil G, Powell A, Gildein H, Geva T. Gadolinium-enhanced three-dimensional magnetic resonance angiography of pulmonary and systemic venous anomalies. *J Am Coll Cardiol* 2002;39:335–41.
11. Valsangiacomo E, Levasseur S, McCrindle B, MacDonald C, Smallhorn J, Yoo S. Contrast-enhanced MR angiography of pulmonary venous abnormalities in children. *Pediatr Radiol* 2003;33:92–8.
12. Shors S, Cotts W, Pavlovic-Surjancev B, Francois C, Gheorghide M, Finn J. Heart failure: evaluation of cardiopulmonary transit times with time-resolved MR angiography. *Radiology* 2003;229:743–8.
13. Pruessmann K, Weiger M, Scheidegger M, Boesiger P. SENSE: sensitivity encoding for fast MRI. *Magn Reson Med* 1999;42:952–62.
14. Ohno Y, Kawamitsu H, Higashino T, Takenaka D, Watanabe H, van CM, et al. Time-resolved contrast-enhanced pulmonary MR angiography using sensitivity encoding (SENSE). *J Magn Reson Imaging* 2003;17:330–6.
15. Sodickson D, Manning W. Simultaneous acquisition of spatial harmonics (SMASH): fast imaging with radiofrequency coil arrays. *Magn Reson Med* 1997;38:591–603.
16. Fink C, Ley S, Kroecker R, Requardt M, Kauczor H, Bock M. Time-resolved contrast-enhanced three-dimensional magnetic resonance angiography of the chest: combination of parallel imaging with view sharing (TREAT) [In Process Citation]. *Invest Radiol* 2005;40:40–8.
17. Schoenberg S, Bock M, Floemer F, Grau A, Williams D, Laub G, et al. High-resolution pulmonary arterio- and venography using

- multiple-bolus multiphase 3D-Gd-mRA. *J Magn Reson Imaging* 1999;10:339–46.
18. Fink C, Eichhorn J, Kiessling F, Bock M, Delorme S. [Time-resolved multiphasic 3D MR angiography in the diagnosis of the pulmonary vascular system in children]. *Rofo Fortschr Geb Rontgenstr Neuen Bildgeb Verfahr* 2003;175:929–35.
 19. Fink C, Puderbach M, Ley S, Plathow C, Bock M, Zuna I, Kauczor H. Contrast-enhanced three-dimensional pulmonary perfusion magnetic resonance imaging: intraindividual comparison of 1.0 M gadobutrol and 0.5 M Gd-DTPA at three dose levels. *Invest Radiol* 2004;39:143–8.
 20. Hoogeveen R, von Falkenhausen M, Gieseke J. Fast dynamic, high resolution contrast-enhanced MR angiography with CEN-TRA keyhole and SENSE. *Proc Intl Soc Mag Reson Med* 11. 2004.
 21. Willinek W, Gieseke J, Conrad R, Strunk H, Hoogeveen R, von FM, et al. Randomly segmented central k-space ordering in high- spatial-resolution contrast-enhanced MR angiography of the supraaortic arteries: initial experience. *Radiology* 2002;225:583–8.
 22. Hendrick RE, Raff U. Image Contrast and Noise. In: Stark D, Bradley W (eds). *Magnetic Resonance Imaging*. Mosby Year Book, St. Louis, 1992: pp 109–44.
 23. Bland J, Altman D. Statistical methods for assessing agreement between two methods of clinical measurement. *Lancet* 1986;1:307–10.
 24. Altman D. *Practical statistics for medical research*. London: Chapman & Hall;1991.
 25. Dill T, Neumann T, Ekinci O, Breidenbach C, John A, Erdogan A, et al. Pulmonary vein diameter reduction after radiofrequency catheter ablation for paroxysmal atrial fibrillation evaluated by contrast-enhanced three-dimensional magnetic resonance imaging. *Circulation* 2003;107:845–50.
 26. Hansen M, Kozerke S, Pruessmann K, Boesiger P, Pedersen E, Tsao J. On the influence of training data quality in k-t BLAST reconstruction. *Magn Reson Med* 2004;52:1175–83.
 27. Syed MA, Peters DC, Rashid H, Arai AE. Pulmonary vein imaging: comparison of 3D magnetic resonance angiography with 2D cine MRI for characterizing anatomy and size. *J Cardiovasc Magn Reson* 2005;7:355–60.